

Learning the Basis: A Kolmogorov-Arnold Network Approach Embedding Green's Function Priors

Rui Zhu, *Student Member, IEEE*, Yuexing Peng, *Member, IEEE*,
 George C. Alexandropoulos, *Senior Member, IEEE*, Wenbo Wang *Senior Member, IEEE*,
 and Wei Xiang *Senior Member, IEEE*

Abstract—The Method of Moments (MoM) is constrained by the usage of static, geometry-defined basis functions, such as the Rao-Wilton-Glisson (RWG) basis. This letter reframes electromagnetic modeling around a learnable basis representation rather than solving for the coefficients over a fixed basis. We first show that the RWG basis is essentially a static and piecewise-linear realization of the Kolmogorov-Arnold representation theorem. Inspired by this insight, we propose PhyKAN, a physics-informed Kolmogorov-Arnold Network (KAN) that generalizes RWG into a learnable and adaptive basis family. Derived from the EFIE, PhyKAN integrates a local KAN branch with a global branch embedded with Green's function priors to preserve physical consistency. It is demonstrated that, across canonical geometries, PhyKAN achieves sub- 10^{-2} reconstruction errors as well as accurate, unsupervised radar cross section predictions, offering an interpretable, physics-consistent bridge between classical solvers and modern neural network models for electromagnetic modeling.

Index Terms—Electromagnetic modeling, method of moments, Kolmogorov-Arnold network, electric field integral equation, adaptive basis functions.

I. INTRODUCTION

SOLVING electromagnetic (EM) scattering via the Electric Field Integral Equation (EFIE) is central to computational electromagnetics (CEM) [1], with the Method of Moments (MoM) being the standard approach. This method expands the induced surface current using predefined basis functions, typically the Rao-Wilton-Glisson (RWG) basis [2]. However, these basis functions are fixed by mesh geometry and are inherently static, a fact that prevents them from adapting to the spatial complexity of current distributions. This rigidity reveals a key limitation of MoM, as its basis functions are not learnable and cannot adapt to the underlying physics.

To address the latter limitation, several directions have been explored. Higher-order basis functions enrich MoM expressiveness using higher-degree polynomials [3]–[5], while characteristic or macro-basis constructions improve efficiency through physics-informed domain decomposition [6], [7]. On another front, instead of improving the basis itself, Adaptive Mesh Refinement (AMR) refines the discretization in regions

R. Zhu, Y. Peng, and W. Wang are with the Key Laboratory of Universal Wireless Communication, Ministry of Education, School of Information and Communication Engineering, Beijing University of Posts and Telecommunications, Beijing 100876, China (e-mails: {rayyyy, yxpeng}@bupt.edu.cn).

G. C. Alexandropoulos is with the Department of Informatics and Telecommunications, National and Kapodistrian University of Athens, Panepistimiopolis Ilisia, 16122 Athens, Greece (e-mail: alexandg@di.uoa.gr).

W. Xiang is with the School of Computing, Engineering and Mathematical Sciences, La Trobe University, Melbourne, VIC 3086, Australia (e-mail: w.xiang@latrobe.edu.au).

of high error [8], [9]. Although effective, these approaches remain largely hand-crafted, problem-specific, and fundamentally tied to predefined basis formulations.

Deep learning techniques are recently emerging as efficient tools in CEM problems, mainly along two directions: black-box current or field prediction without any explicit basis representation [10], [11], and MoM acceleration through surrogate models, operator learning, or iterative refinement, still relying on fixed basis functions [12]–[14]. More recent studies integrate physical structure into neural models, such as EFIE-guided graph learning [15], [16]. This indicates that neither direction addresses the non-learnable nature of the basis functions, which remain unable to adapt to EM physics.

Recent progress in scientific machine learning enables neural network architectures that integrate physical structure with learnable representations. The Kolmogorov–Arnold Network (KAN) [17] is one of the well suited learning frameworks for this purpose that replaces fixed activations with learnable univariate functions [18], providing adaptable basis behavior. KAN is flexible in both kernel choices [19], [20] and graph-based extensions [21] that embed geometric and physical interactions, making it a strong foundation for a physics-guided learnable basis for the MoM approach.

In this letter, we reformulate MoM basis construction as a learnable function problem and show that KAN provides a theoretically grounded generalization of the RWG basis. In addition, a physics-guided EFIE-based framework, termed as PhyKAN, that embeds Green's function [22] priors for physically consistent and adaptive current modeling, while remaining compact and interpretable, is introduced. The proposed learning framework accommodates multiple kernel functions and structural extensions, offering a unified bridge between classical integral equation solvers and neural network models.

II. SURFACE CURRENT AS A LEARNING PROBLEM

Let $\mathbf{G}(\cdot) \in \mathbb{C}^{3 \times 3}$ denote the dyadic Green's function in the three-dimensional free space, $\mathbf{J}(\cdot) \in \mathbb{C}^{3 \times 1}$ the induced surface current, and $\mathbf{E}_{\text{inc}}(\cdot) \in \mathbb{C}^{3 \times 1}$ the incident field. By applying the boundary conditions of Perfectly Electrically Conducting (PEC) objects \mathcal{D} , the EFIE can be formulated $\forall \mathbf{p} \in \mathbb{R}^3$ as follows:

$$\int_{\mathbf{p}' \in \mathcal{D}} \mathbf{G}(\mathbf{p}, \mathbf{p}') \mathbf{J}(\mathbf{p}') d\mathbf{p}' = \mathbf{E}_{\text{inc}}(\mathbf{p}). \quad (1)$$

The MoM discretizes this integral equation by expanding the unknown current $\mathbf{J}(\mathbf{p})$ using a set of predefined basis functions. Typically, the RWG basis $\{f_n(\cdot)\}_{n=1}^3$ comprising

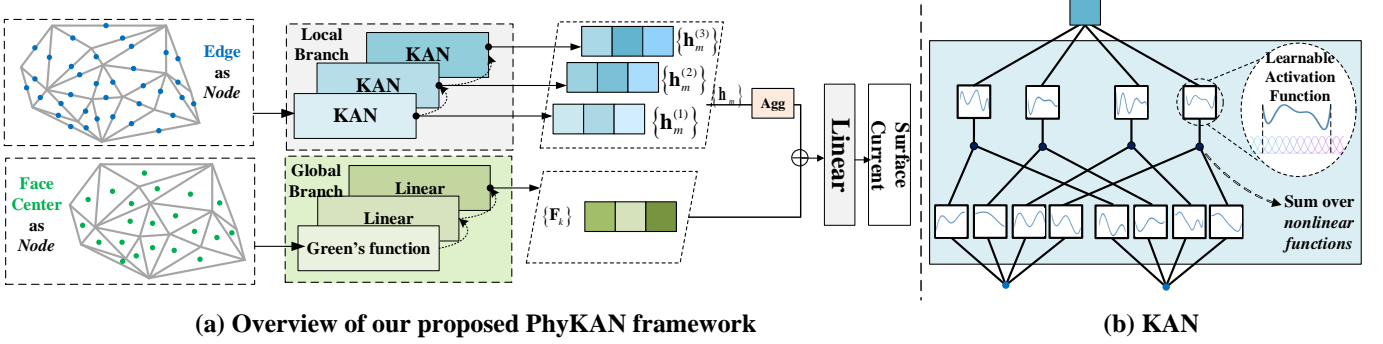


Fig. 1. (a) The architecture of the proposed PhyKAN comprising a local branch that encodes geometric features using a conventional KAN and global branch that incorporates Green's function priors for physically consistent prediction of the induced surface current. (b) The structure of the conventional KAN [17], where learnable activation functions enable adaptive basis modeling.

fixed and geometry-defined functions [2] is used, yielding the following surface current approximation:

$$\mathbf{J}(\mathbf{p}'_k) \approx \sum_{n=1}^3 I_{n,k} f_n(\mathbf{p}'_k), \quad (2)$$

where $I_{n,k}$ are the unknown complex coefficients of the n -th RWG basis function on the k -th triangular element centered at \mathbf{p}'_k . This geometry-fixed basis restricts the MoM's adaptability to complex current distributions. Existing refinements, such as higher-order bases [3]–[5], the characteristic basis function method (CBFM) [7], and AMR [8], [9], partially alleviate this limitation but do not alter the static nature of the basis itself.

Although recent deep learning works [10]–[16] attempt to either learn geometry-to-current mappings or accelerate MoM via surrogate models, they still operate on fixed basis functions, thus leaving the core limitation unresolved. This reveals a fundamental gap: a formulation that preserves the MoM structure while enabling adaptive basis functions is still missing. To this end, instead of solving for $I_{n,k}$ in (2) satisfying the EFIE in (1), we focus on learning an optimal, data-driven basis family $\{b_n(\cdot; \mathbf{u})\}$, yielding the generalized expansion

$$\mathbf{J}(\mathbf{p}'_k) \approx \sum_{n=1}^{N_b} \alpha_{n,k} b_n(\mathbf{p}'_k; \mathbf{u}). \quad (3)$$

Here, N_b denotes the number of learnable basis functions used per element, $\alpha_{n,k}$ is the coefficient associated with the n -th learnable basis on the k -th triangular element, and $b_n(\cdot; \mathbf{u})$ is a learnable function parameterized by \mathbf{u} , whose goal is to adapt its functional shape locally based on the underlying physics and geometry. Notably, setting $b_n = f_n$ and $\alpha_{n,k} = I_{n,k}$ recovers the classical MoM expansion in (2) as a special case.

The latter problem finds its direct mathematical foundation in the Kolmogorov–Arnold representation theorem, which states that any multivariate function can be decomposed into finite sums of univariate functions [23]:

$$f(x_1, \dots, x_d) = \sum_{i=1}^{2d+1} \alpha_i \left(\sum_{j=1}^d \phi_{ij}(x_j) \right), \quad (4)$$

where d is the input dimension, α_i are learnable weights, and $\phi_{ij}(\cdot)$'s are univariate nonlinear mappings. The KAN is the neural network architecture that operationalizes this theorem. Instead of fixed node activations, this network places learnable, spline-based univariate functions $\phi(x)$ on its edges:

$$\phi(x) \triangleq w_b \text{SiLU}(x) + w_s \text{spline}(x), \quad (5)$$

where $\text{SiLU}(x) \triangleq x/(1 + e^{-x})$ provides smooth global nonlinearity and $\text{spline}(x) \triangleq \sum_i c_i B_i(x)$ is a local B -spline expansion with trainable coefficients c_i . Here, w_b and w_s are learnable scalar weights that balance the contributions of the SiLU and spline components, respectively.

To obtain a learnable variant of this formulation, each basis function in (3) is internally parameterized using the KAN-based spline representation in (5). In particular, we express each learnable basis as a linear combination of M spline atoms:

$$b_n(\mathbf{p}'_k; \mathbf{u}) = \sum_{i=1}^M c_i B_i(\mathbf{p}'_k), \quad (6)$$

where $B_i(\cdot)$ denotes the i -th spline atom of the n -th basis (initialized as first-order B -splines) and $c_{n,i}$ are its learnable weights. Substituting (6) into (3) yields

$$\mathbf{J}(\mathbf{p}'_k) \approx \sum_{n=1}^{N_b} \sum_{i=1}^M \alpha_{n,k} c_{n,i} B_{n,i}(\mathbf{p}'_k). \quad (7)$$

To more closely mirror the MoM form in (2), we absorb the coefficient into the spline weights via $\tilde{c}_{n,i,k} \triangleq \alpha_{n,k} c_{n,i}$ which produces the following compact, MoM-consistent current expansion can be expressed as

$$\mathbf{J}(\mathbf{p}'_k) \approx \sum_{(n,i)} \tilde{c}_{n,i,k} B_{n,i}(\mathbf{p}'_k), \quad (8)$$

where the summation $\sum_{(n,i)}$ runs over all $n = 1, \dots, N_b$ and $i = 1, \dots, M$. Expression (8) is structurally isomorphic to the MoM formulation in (2), with $\tilde{c}_{n,i,k}$ acting as the learnable counterpart of $I_{n,k}$ and $B_{n,i}$ serving as data-driven, adaptive generalizations of the fixed RWG basis functions. Critically, unlike MoM, which only solves for $I_{n,k}$ against a fixed basis $\{f_n(\cdot)\}_{n=1}^3$, We thus regard KAN as a learnable generalization of the RWG basis, preserving the MoM structure while enabling physics-adaptive basis functions.

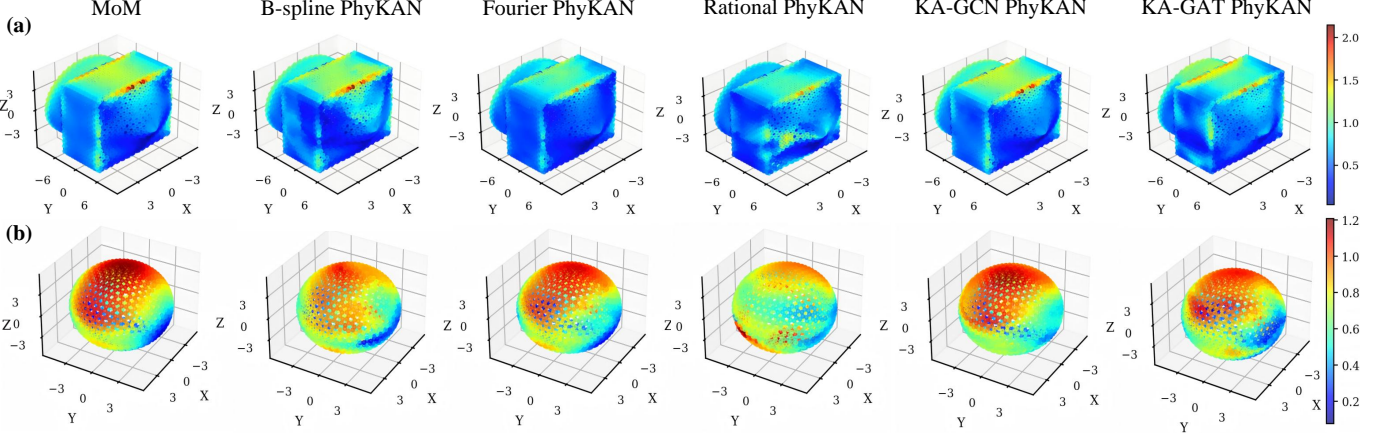


Fig. 2. Reconstruction results for the surfaces of two objects with different variants of the proposed two-branch PhyKAN architecture.

III. PROPOSED PHYKAN FRAMEWORK

In this section, we build upon the preceding formulation that recasts the MoM basis functions into a learnable KAN-based representation, and introduce PhyKAN, a physics-guided learning framework derived from the EFIE. The proposed network, whose architecture is visualized in Fig. 1(a), has a dual-branch structure that enables adaptive basis learning by separately modeling local geometric features and global EM interactions.

A. Neural Network Architecture

The **local branch** learns edge-wise basis representations by treating each RWG basis function as a node, consistent with MoM where an RWG basis is defined on the shared edge of two triangular faces. The input is a set of M edge-nodes, each described by a geometric feature vector $\mathbf{g}_m \in \mathbb{R}^d$ encoding local geometry, where d is the dimension of the feature vector that encodes local geometric information. As shown in Fig. 1(a), this descriptor is then mapped through a KAN block to produce a latent feature vector, as follows:

$$\mathbf{h}_m^{(l)} \triangleq \text{KAN}_u(\mathbf{g}_m). \quad (9)$$

where $\mathbf{h}_m^{(l)} \in \mathbb{R}^D$ denotes the l -th layer embedding. As shown in Fig. 1(b), each KAN layer uses spline-based learnable activations (with optional B-spline or Fourier kernels) to enable adaptive basis shaping. The outputs of the three layers are fused to form the complete latent representation of each edge embedding \mathbf{h}_m , which serves as the learned local counterpart of the conventional RWG basis.

The local feature \mathbf{H}_k of each k -th element-node is aggregated from its three associated edge local embeddings of the corresponding edges (\mathbf{h}_a , \mathbf{h}_b , and \mathbf{h}_c), as follows:

$$\mathbf{H}_k = \frac{1}{3}(\mathbf{h}_a + \mathbf{h}_b + \mathbf{h}_c), \quad (10)$$

providing a learnable counterpart of the RWG basis local expansion.

The **global branch** of PhyKAN models long-range electromagnetic interactions across the surface. In contrast to the local branch where each node corresponds to a mesh edge, here one

element-node is defined per triangular element. The input to this branch is a set of K element-nodes, where each node k is represented by the centroid $\mathbf{p}_k \in \mathbb{R}^3$ of the k -th element, together with the incident direction (θ, ϕ) of the scattered EM fields $\mathbf{E}_{\text{inc}}(\mathbf{p}_k)$'s. To incorporate EM priors into this branch, we initialize the weights of its first layer, $\mathbf{W}_{k,j}^{(0)} \in \mathbb{R}^{K \times K}$, using the dyadic Green's function, as follows:

$$\mathbf{W}_{k,j}^{(0)} = \mathbf{G}(\mathbf{p}_k, \mathbf{p}_j), \quad (11)$$

which encodes the physical interaction between element-nodes k and j . To incorporate the dependence on incidence, the incident angles (θ, ϕ) are mapped into a D_{ang} -dimensional Fourier embedding:

$$\gamma(\theta, \phi) = [\sin(\omega_1 \theta), \cos(\omega_1 \theta), \dots, \sin(\omega_L \phi), \cos(\omega_L \phi)], \quad (12)$$

where $\{\omega_\ell\}_{\ell=1}^L$ are frequency parameters and $D_{\text{ang}} = 4L$. In the sequel, the global coupling features and the latter D_{ang} -directional embedding are concatenated and sequentially passed through two linear projections, yielding:

$$\mathbf{F}_k = \mathbf{W}^{(2)} \left(\sigma \left(\mathbf{W}^{(1)} \left(\sum_{j=1}^K \mathbf{W}_{kj}^{(0)} \mathbf{p}_j \right) \oplus \gamma(\theta, \phi) \right) \right) + \mathbf{b}, \quad (13)$$

where \oplus denotes concatenation, $\sigma(\cdot)$ is an activation, and $\mathbf{W}^{(1)}$, $\mathbf{W}^{(2)}$, and \mathbf{b} are trainable parameters.

To predict surface currents, the local basis feature \mathbf{H}_k and the global physical context \mathbf{F}_k :

$$\mathbf{z}_k = \mathbf{H}_k \oplus \mathbf{F}_k, \quad (14)$$

and projected to the 6-dimensional output $\mathbf{J}_{\text{pre}}(\mathbf{p}_k) \in \mathbb{C}^{3 \times 1}$ via a linear head.

B. Physics-Informed Loss Function

Instead of directly minimizing the difference between predicted and reference currents, we adopt a residual-based loss function derived directly from the EFIE, which is defined as:

$$L = \frac{1}{N_s} \sum_{u=1}^{N_s} \left\| \sum_{j=1}^K \mathbf{G}(\mathbf{p}_k, \mathbf{p}_j) \mathbf{J}_{\text{pre}}(\mathbf{p}_k) - \mathbf{E}_{\text{inc}}(\mathbf{p}_k) \right\|_2^2, \quad (15)$$

TABLE I
OUR PROPOSED PHYKAN FRAMEWORK'S RECONSTRUCTION PERFORMANCE.

Dataset	Cube	Sphere	Cone	Assembly Body
B-spline PhyKAN	0.0098	0.0089	0.0084	0.0092
Fourier PhyKAN	0.0123	0.0072	0.0101	0.0104
Rational PhyKAN	0.0115	0.0107	0.0119	0.0145
KA-GCN PhyKAN	0.0061	0.0075	0.0060	0.0064
KA-GAT PhyKAN	0.0107	0.0119	0.0079	0.0088

TABLE II
GREEN'S FUNCTION INITIALIZATION (INIT.) ABLATION FOR THE ASSEMBLY BODY RECONSTRUCTION.

Kernel	MSE (no init.)	MSE (Green init.)
KA-GCN PhyKAN	0.0123	0.0064
KA-GAT PhyKAN	0.0191	0.0088

where N_s is the batch size and p_k is the center of the k -th triangular mesh element. This loss enforces the predicted surface currents to satisfy the EFIE, thereby ensuring physical consistency without requiring any supervised labels.

IV. NUMERICAL RESULTS AND DISCUSSION

To evaluate PhyKAN, MoM solutions are used as ground-truth for current reconstruction and RCS validation. The model inputs triangular mesh elements with EM descriptors and outputs induced currents. Tests are performed on four canonical PEC shapes [16] (cube, sphere, cone, assembly body) under a 1 GHz, unit-amplitude, vertical plane wave with $\theta, \phi \in [0^\circ, 180^\circ]$. Five variants assess the effect of KAN designs: three kernel activations (B-spline, Fourier, Rational) [18]–[20] and two graph KAN extensions (KA-GCN, KA-GAT) [21], used interchangeably in the local KAN blocks. Each is denoted *[Kernel/Graph]-PhyKAN*. DL-based CEM baselines either black-box the current mapping or only accelerate MoM without learnable bases; hence, we benchmark PhyKAN variants under a unified setting against MoM.

Figure 2 visualizes the surface reconstruction capability of five different variants of the proposed two-branch PhyKAN architecture. As observed, on the smooth geometry of the sphere, Fourier and KA-GCN PhyKAN accurately recover the global current distribution, while the *B*-spline and KA-GCN variants better capture sharp-edge behaviors on complex assemblies through localized and hierarchical aggregation. Quantitatively, Table I summarizes the mean-squared error (MSE) of each PhyKAN variant with respect to the MoM reference on the cube, sphere, cone, and assembly datasets. All variants show low reconstruction error against MoM, and the Fourier and KA-GCN configurations consistently achieve the highest accuracy across the canonical geometries. These results confirm that PhyKAN serves as a learnable, physics-adaptive basis, effectively overcoming the static rigidity of traditional RWG representations. This is actually attributed to its capability to tailor its current representation to the underlying geometry and field physics.

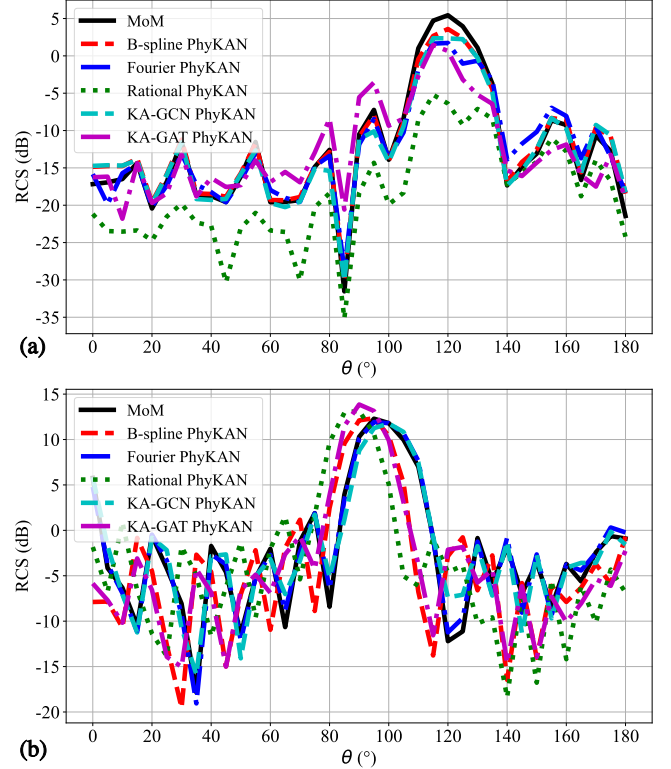


Fig. 3. Bistatic RCS at $\phi = 0^\circ$ for (a) the cube and (b) the cone objects, comparing different PhyKAN variants against the MoM reference.

To further assess the physical fidelity of the learned surface currents, the radar cross section (RCS) [24] is computed as a downstream validation in Fig. 3. It is shown that the predicted RCSs with all five considered PhyKAN variants agrees well with MoM references for both the cube and cone, even though this metric was never included as a training objective. This demonstrates that PhyKAN generalizes from near-field currents to physically consistent far-field responses, validating its physical consistency and confirming it avoids non-generalizable, black-box behavior.

In Table II, an ablation study, considering the assembly body, that directly validates the Phy- component of the proposed PhyKAN framework is included. It can be seen that using Green's function initialization significantly reduces reconstruction error. This confirms that embedding this physical prior is essential, strengthening both model accuracy and physical consistency. Overall, the results confirm that PhyKAN delivers geometry-adaptive and physically consistent surface current modeling, unifying data-driven flexibility with EM rigor.

V. CONCLUSION

This letter introduced PhyKAN, a physics-guided EFIE-derived framework that enables a learnable basis for EM modeling. By generalizing the RWG basis into an adaptive and interpretable representation, the proposed PhyKAN framework unifies diverse kernel and structural extensions within a physically consistent architecture. Future work will focus on scaling the learnable basis to large-scale and broadband scenarios.

REFERENCES

- [1] S. M. Rao, D. R. Wilton, and A. W. Glisson, "Electromagnetic scattering by surfaces of arbitrary shape," *IEEE Trans. Antennas Propag.*, vol. 30, no. 3, pp. 409–418, May 1982.
- [2] R. F. Harrington and J. L. Harrington, *Field Computation by Moment Methods*. Oxford, U.K.: Oxford Univ. Press, Inc., 1996.
- [3] G. Kang, J. Song, W. C. Chew, K. C. Donepudi, and J.-M. Jin, "A novel grid-robust higher order vector basis function for the method of moments," *IEEE Trans. Antennas Propag.*, vol. 49, no. 6, pp. 908–915, Jun. 2001.
- [4] O. S. Kim and P. Meincke, "Adaptive integral method for higher order method of moments," *IEEE Trans. Antennas Propag.*, vol. 56, no. 8, pp. 2298–2305, Aug. 2008.
- [5] N. Zhang, Y. Chen, Y. Ren, and J. Hu, "A modified HODLR solver based on higher order basis functions for solving electromagnetic scattering problems," *IEEE Antennas Wireless Propag. Lett.*, vol. 21, no. 12, pp. 2452–2456, Dec. 2022.
- [6] E. Lucente, A. Monorchio, and R. Mittra, "An iteration-free MoM approach based on excitation independent characteristic basis functions for solving large multiscale electromagnetic scattering problems," *IEEE Trans. Antennas Propag.*, vol. 56, no. 4, pp. 999–1007, Apr. 2008.
- [7] P. Du, Z.-W. Tong, H. Lin, and G. Zheng, "Wideband RCS analysis of finite periodic array in the vicinity of object using modified SSED-CBFM and improved FIR," *IEEE Antennas Wireless Propag. Lett.*, vol. 24, no. 6, pp. 1447–1451, Jun. 2025.
- [8] T. Plewa, T. Linde, and V. G. Weirs, Eds., *Adaptive Mesh Refinement: Theory and Applications*, Proc. Chicago Workshop on Adaptive Mesh Refinement Methods, Sep. 3–5, 2003. Berlin, Germany: Springer, 2005.
- [9] A. Amor-Martin and L. E. Garcia-Castillo, "Adaptive semi-structured mesh refinement techniques for the finite element method," *Appl. Sci.*, vol. 11, no. 8, p. 3683, Apr. 2021.
- [10] J. H. Kim and S. W. Choi, "A deep learning-based approach for radiation pattern synthesis of an array antenna," *IEEE Access*, vol. 8, pp. 226059–226063, 2020.
- [11] M. Salucci, M. Arrebola, T. Shan, and M. Li, "Artificial intelligence: New frontiers in real-time inverse scattering and electromagnetic imaging," *IEEE Trans. Antennas Propag.*, vol. 70, no. 8, pp. 6349–6364, Aug. 2022.
- [12] M. Baldan, P. Di Barba and D. A. Lowther, "Physics-informed neural networks for inverse electromagnetic problems," *IEEE Trans. Magn.*, vol. 59, no. 5, pp. 1–5, May 2023.
- [13] C. Brennan and K. McGuinness, "Site-specific deep learning path loss models based on the method of moments," *Proc. 17th Eur. Conf. Antennas Propag. (EuCAP)*, Florence, Italy, 2023.
- [14] D.-H. Kong, J.-N. Cao, W.-W. Zhang, W.-C. Huang, X.-Y. He and L. Liu, "An AI predictor: From point clouds to scattered far fields for 3-D PEC targets," *IEEE Trans. Antennas Propag.*, vol. 72, no. 6, pp. 5179–5190, Jun. 2024.
- [15] K. Stylianopoulos, P. Gavriilidis, G. Gradoni, and G. C. Alexandropoulos, "Graph-CNNs for RF imaging: Learning the electric field integral equations," in *Proc. European Signal Process. Conf. (EUSIPCO)*, Palermo, Italy, Sep. 2025, pp. 1–5.
- [16] R. Zhu, Y. Peng, P. Wang, G. C. Alexandropoulos, W. Wang, and W. Xiang, "U-PINet: End-to-end hierarchical physics-informed learning with sparse graph coupling for 3D EM scattering modeling," *arXiv preprint arXiv:2508.03774*, Aug. 2025.
- [17] Z. Liu, Y. Wang, S. Vaidya, F. Ruehle, J. Halverson, M. Soljačić, T. Y. Hou, and M. Tegmark, "KAN: Kolmogorov–Arnold networks," in *Proc. 13th Int. Conf. Learn. Represent. (ICLR)*, Singapore, Apr. 2025, pp. 1346–1354.
- [18] J. D. Toscano, V. Oomen, A. J. Varghese, Z. Zou, N. A. Daryakenari, C. Wu, and G. E. Karniadakis, "From PINNs to PIKANs: Recent advances in physics-informed machine learning," *Mach. Learn. Comput. Sci. Eng.*, vol. 1, no. 15, Mar. 2025.
- [19] J. Xu, Z. Chen, J. Li, S. Yang, W. Wang, X. Hu, and E. C. H. Ngai, "FourierKAN-GCF: Fourier Kolmogorov–Arnold network– An effective and efficient feature transformation for graph collaborative filtering," *CoRR*, vol. abs/2406.01034, 2024.
- [20] X. Yang and X. Wang, "Kolmogorov–Arnold Transformer," in *Proc. Int. Conf. Learn. Represent. (ICLR)*, Singapore, Apr. 2025, pp. 76063–76086.
- [21] L. Li, Y. Zhang, G. Wang, and K. Xia, "Kolmogorov–Arnold graph neural networks for molecular property prediction," *Nat. Mach. Intell.*, vol. 7, pp. 1346–1354, Aug. 2025.
- [22] G. Barton, *Elements of Green's Functions and Propagation: Potentials, Diffusion, and Waves*. Oxford, U.K.: Clarendon Press, 1989, p. 465.
- [23] A. N. Kolmogorov, "On the representation of continuous functions of several variables as superpositions of continuous functions of a smaller number of variables," *Dokl. Akad. Nauk SSSR*, vol. 108, no. 2, pp. 179–182, 1956.
- [24] M. A. Richards, *Fundamentals of Radar Signal Processing*, 2nd ed. New York, NY, USA: McGraw-Hill, 2014.